



A new DOA estimation algorithm for wideband signals in the presence of unknown spatially correlated noise

P. Palanisamy^{a,*}, N. Kalyanasundaram^b, A. Raghunandan^c

^a Department of Electronics and Communication, National Institute of Technology, Tiruchirappalli 620015, India

^b Department of Electronics and Communication, JIIT University, Noida 201307, India

^c CISCO Systems, Bangalore 560087, India

ARTICLE INFO

Article history:

Received 20 July 2008

Received in revised form

23 March 2009

Accepted 23 March 2009

Available online 8 April 2009

Keywords:

Wideband

Direction-of-arrival

Forward–backward averaging

Spatially correlated noise

Propagator

ABSTRACT

In this paper, a new high resolution direction-of-arrival (DOA) estimation technique is proposed for wideband signals in the presence of spatially correlated noise with unknown covariance matrix. The proposed technique is based on the (matrix) difference between the forward–backward averaged covariance matrix of the observations and the Hermitian of the backward covariance matrix of the observations. This differencing operation eliminates the noise covariance matrix from the difference matrix. The propagator method is then applied to the difference matrix to find the DOA. This proposed technique does not require any initial estimate of the DOAs and is effective for both correlated and partially correlated sources. In this paper, the proposed technique is applied to a uniform linear array and an L-shaped array for both one- and two-dimensional DOA estimation. Simulations results comparing the performance of the proposed method with that of the coherent propagator method are presented.

© 2009 Elsevier B.V. All rights reserved.

1. Introduction

Direction-of-arrival (DOA) estimation is one of the important research areas of array signal processing [1], which has been attracting the attention of the signal processing community for more than three decades. DOA is one of the most important parameters that needs to be estimated in many applications. For radar, DOA estimation is the most important operation performed to localize targets. For communications, DOA estimation can give spatial diversity to the receiver to enable multi-user scenarios. There exists at present a large number of algorithms for DOA estimation. Signal subspace methods are very well known DOA estimation techniques with high performance and relatively low computational cost.

MUSIC (MULTiple Signal Classification) [2] and ESPRIT [3] fall into this category. Most of these methods take advantage of the fact that there is only a phase difference among the different sensor outputs, when the signals are narrowband. Therefore, the subspace methods work exclusively under this narrowband assumption.

Recently, wideband signals have attracted considerable attention because of their inherent advantages over narrowband signals in applications such as radar, sonar, seismology, and spread spectrum communications. For example, ultra wideband (UWB) radar can provide high resolution images [4], and UWB wireless communication can counteract the effects of channel fading due to multipath [5]. Wideband signals are also used to track moving objects from acoustic measurements [6] or to find buried objects with the help of seismic sensors [7]. Use of wideband signals results in high data rates in communication.

Direct exploitation of raw wideband signals for DOA estimation using the traditional narrowband technique leads to failure. The reason is that the narrowband

* Corresponding author.

E-mail addresses: palan@nitt.edu (P. Palanisamy), n.kalyanasundaram@jiit.ac.in (N. Kalyanasundaram), raghunandan.403@gmail.com (A. Raghunandan).

methods, which require the bandwidth to be small, exploit the fact that time delays directly translate to phase differences so long as the phase remains approximately constant over the bandwidth. On the other hand, for wideband signals, whose bandwidth is not small compared to the centre frequency, this direct proportionality between time delays and phase differences does not hold.

One simple way to deal with wideband signals is to decompose the wideband signal into many narrowband signals centered around frequencies with large power concentration using filter banks or the discrete Fourier transform in the temporal domain [8–10]. Narrowband methods can then be applied to each narrowband component of the decomposed signal. However, this kind of approach does not take advantage of the signal's full frequency band because of the possibility of rejecting some frequency bins, which might have had information about the DOA, on the basis of the power-concentration criterion. These methods, which apply narrowband processing to the selected frequency bins independently, are called incoherent methods. Several different approaches that make full use of all the frequency components of a wideband signal in a coherent fashion have been published in the literature [11–15]. Most of these coherent methods involve a conversion of wideband data or statistics into narrowband forms, either directly or indirectly, so that narrowband subspace methods become applicable. One of the most well-known of coherent methods is the coherent signal subspace method (CSSM) [16] from which many other variants derive their roots [17–19]. CSSM requires a preprocessing step called focusing. The focusing step requires an initial estimate of the DOAs which should be as close as possible to the true DOAs. If the initial values are substantially different from the true DOAs, the DOA estimate could exhibit a bias that does not vanish as the number of data samples approaches infinity [20].

Most of the high resolution techniques for estimating DOAs have been applied to spatially white noise models [2,3]. For the case of non-white (correlated) noise, the noise-covariance matrix is assumed to be known, but in reality, estimating the noise covariance matrix may be a problem. Many algorithms [21] have been proposed to solve this problem assuming uncorrelated sources. The drawbacks of these algorithms, in the presence of spatially correlated noise fields, are (i) an increase in the bias of the DOA estimate and hence a degradation in performance and (ii) the need for a computationally intensive eigen-decomposition of the covariance matrix of the observations to find the DOAs. In this context, the so-called propagator method, which does not require eigen-decomposition, proposed by Marcos et al. [22], is quite attractive from the computational point of view. But the performance of the propagator method (PM) is poor when the signal-to-noise ratio (SNR) is low. The PM cannot significantly reduce the effects of unknown noise because the PM requires noise covariance matrices to be known.

In this paper, a high resolution DOA estimation technique based on differencing the forward-backward (FB) averaged covariance matrix and the Hermitian of

backward covariance matrix [20] for a uniform linear array (ULA) and an L-shaped array for wideband sources in the presence of unknown spatially correlated noise is presented. The PM is then applied to the difference matrix and the resulting incoherent propagator matrices are then transformed using certain focusing matrices. Finally, a coherent propagator matrix is obtained by averaging the transformed incoherent propagator matrices. The coherent propagator matrix is then used to estimate the DOAs of wideband sources.

For the DOA estimation problem in the presence of an unknown correlated noise field addressed in this paper, the noise-covariance matrix is assumed to be in the Hermitian symmetric Toeplitz form as in [23,24]. This assumption is justified when the noise field is cylindrically or spherically isotropic around the array elements. Such a situation is typically encountered when the noise field is radiated by a set of point sources distributed symmetrically about the array broadside [23]. This is the type of noise that would be encountered in a passive sonar environment when wind-generated noise is dominant [25].

The paper is organized as follows: In Section 2, the data models for a uniform linear array and an L-shaped array are presented. In Section 3, the proposed DOA algorithm for wideband signals is derived. In Section 4, we present numerical simulations that illustrate the mean-square error reduction and resolution improvement achieved by the proposed method as compared to the coherent propagator method. Finally, Section 5 concludes the paper.

Throughout this paper, vectors are denoted by lowercase bold letters and matrices by uppercase bold letters. The superscripts *, T and H denote, respectively, complex conjugation, transposition, and conjugate transposition.

2. Formulation of data models

2.1. Data model for a uniform linear array

Consider a uniform linear array consisting of M sensors, with inter-element spacing d , that receives the wave field radiated by K wideband sources in the presence of an arbitrary noise field. It is assumed that the number K of such sources has already been estimated using one of the standard methods [26–28]. The received signals are assumed to be zero-mean, wide-sense stationary random processes band-limited to W over the finite observation interval. The DOA of the k th source signal is θ_k for $k = 1, 2, \dots, K$, with respect to the array normal. The observation interval is subdivided into D disjoint intervals. The received signal $\tilde{z}_m(t)$ at the m th sensor, in each sub-interval, can be written as

$$\tilde{z}_m(t) = \sum_{k=1}^K \tilde{s}_k(t - \tau_m(\theta_k)) + \tilde{\eta}_m(t), \quad (1)$$

where $\tilde{s}_k(t)$ is the k th source signal, $\tilde{\eta}_m(t)$ is the noise observed at the m th sensor, and $\tau_m(\theta_k) = ((m-1)d \cos \theta_k/c)$ is the relative delay where c is the constant propagation speed of the source signals.

The sampled signal at the m th sensor in each sub-interval is decomposed into N narrowband components $z_m(\omega_n)$, $n = 0, 1, \dots, N-1$, using DFT. The resulting narrowband components corresponding to any one of the sub-intervals may be expressed as

$$z_m(\omega_n) = \sum_{k=1}^K s_k(\omega_n) \exp(-j\omega_n \tau_m(\theta_k)) + \eta_m(\omega_n) \quad (2)$$

for $m = 1, 2, \dots, M$ and $n = 0, 1, \dots, N-1$,

where $s_k(\omega_n)$ is the n th (radian) frequency component of the source signal $\tilde{s}_k(t)$ and $\eta_m(\omega_n)$ is n th frequency component of the noise process $\tilde{\eta}_m(t)$. Denoting the $M \times 1$ observation vector corresponding to the n th frequency $f_n(\Delta\omega_n/2\pi)$ by $\mathbf{z}(\omega_n) = [z_1(\omega_n), z_2(\omega_n), \dots, z_M(\omega_n)]^T$, (2) can be expressed as

$$\mathbf{z}(\omega_n) = \mathbf{A}(\omega_n)\mathbf{s}(\omega_n) + \boldsymbol{\eta}(\omega_n) \quad \text{for } n = 0, 1, \dots, N-1, \quad (3)$$

where

$$\mathbf{A}(\omega_n) = [\mathbf{a}(\theta_1, \omega_n), \mathbf{a}(\theta_2, \omega_n), \dots, \mathbf{a}(\theta_K, \omega_n)]$$

is the $M \times K$ steering matrix at the n th frequency f_n ,

$$\mathbf{s}(\omega_n) = [s_1(\omega_n), s_2(\omega_n), \dots, s_K(\omega_n)]^T,$$

and

$$\boldsymbol{\eta}(\omega_n) = [\eta_1(\omega_n), \eta_2(\omega_n), \dots, \eta_M(\omega_n)]^T,$$

and where

$$\mathbf{a}(\theta_k, \omega_k) = [\exp(-j\omega_n \tau_1(\theta_k)), \dots, \exp(-j\omega_n \tau_M(\theta_k))]^T \quad \text{for } k = 1, 2, \dots, K.$$

Assuming that the noise is uncorrelated with the source signals, the covariance matrix $\mathbf{R}_z(\omega_n)$ of the observation vector $\mathbf{z}(\omega_n)$ at the n th frequency f_n is given by

$$\mathbf{R}_z(\omega_n) = \mathbf{A}(\omega_n)\mathbf{R}_s(\omega_n)\mathbf{A}^H(\omega_n) + \mathbf{Q}_\eta(\omega_n) \quad \text{for } n = 0, 1, \dots, N-1, \quad (4)$$

where $\mathbf{R}_s(\omega_n)$ and $\mathbf{Q}_\eta(\omega_n)$ denote, respectively, the signal covariance matrix and the noise covariance matrix at the frequency f_n .

2.2. Data model for an L-shaped array

Fig. 1 shows the L-shaped configuration of the array as lying on the x - z plane. Each of the two mutually perpendicular linear sub-arrays consists of M elements. Assume that there are K wideband signals $\tilde{s}_1(t), \tilde{s}_2(t), \dots, \tilde{s}_K(t)$ arriving at the L-shaped array, respectively, from the directions $(\theta_1, \varphi_1), (\theta_2, \varphi_2), \dots, (\theta_K, \varphi_K)$, where θ_k and φ_k , for $k = 1, 2, \dots, K$, are, respectively, the elevation angle and azimuthal angle of the k th signal $\tilde{s}_k(t)$. The superposition $\tilde{s}(t)$ of these K wideband signals received by the array in the presence of an unknown noise field is processed by considering the L-shaped array to be made up of two independent ULAs (one along the z -axis and the other along the x -axis). The DOAs of the received wideband signal are determined by first estimating the elevation θ_k using the ULA on the z -axis and then, for this θ_k , the azimuthal angle φ_k is estimated using the ULA on the x -axis. For the ULA on the z -axis, the data model is the same

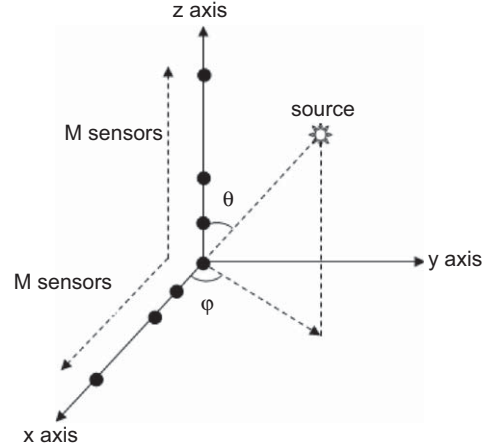


Fig. 1. L-shaped array configuration.

as that discussed in Section 2.1. Thus, the 2-D DOAs of the received signal $\tilde{s}(t)$ are determined by automatic pair matching.

For the ULA on the x -axis, the projection of the observation vector at n th frequency f_n on the x -axis can be written as

$$\mathbf{x}(\omega_n) = \mathbf{A}(\omega_n)\mathbf{s}(\omega_n) + \boldsymbol{\eta}_x(\omega_n) \quad (5)$$

where

$$\mathbf{A}(\omega_n) = [\mathbf{a}(\theta_1, \varphi_1, \omega_n), \mathbf{a}(\theta_2, \varphi_2, \omega_n), \dots, \mathbf{a}(\theta_K, \varphi_K, \omega_n)]$$

is an $M \times K$ steering matrix at f_n and $\boldsymbol{\eta}_x(\omega_n)$ is the projected $M \times 1$ noise vector and where

$$\mathbf{a}(\theta_k, \varphi_k, \omega_n) = [\exp(-j\omega_n \tau_1(\theta_k, \varphi_k)), \dots, \exp(-j\omega_n \tau_M(\theta_k, \varphi_k))]^T \quad \text{for } k = 1, 2, \dots, K,$$

using $\tau_m(\theta_k, \varphi_k)$ to denote the relative delay $(m-1)d \sin \theta_k \cos \varphi_k / c$ at the m th sensor for $m = 1, 2, \dots, M$. From (5), the covariance matrix $\mathbf{R}_x(\omega_n)$ of $\mathbf{x}(\omega_n)$ can be expressed in terms of the signal-covariance matrix $\mathbf{R}_s(\omega_n)$ and the noise-covariance matrix $\mathbf{Q}_{\eta_x}(\omega_n)$ as

$$\mathbf{R}_x(\omega_n) = \mathbf{A}(\omega_n)\mathbf{R}_s(\omega_n)\mathbf{A}^H(\omega_n) + \mathbf{Q}_{\eta_x}(\omega_n). \quad (6)$$

2.3. Steps for data modeling of wideband sources

Step 1: Divide the sensor output data into D identically sized non-overlapping blocks of length L .

Step 2: Compute the temporal L-point DFT $\mathbf{y}_d(\omega_n)$ at the n th (radian) frequency ω_n ($n = 0, 1, \dots, N-1$) where $\mathbf{y}_d(\omega_n)$ ($= \mathbf{z}(\omega_n)$ or $\mathbf{x}(\omega_n)$) is the snap-shot vector at ω_n corresponding to the d th ($d = 1, 2, \dots, D$) block.

Step 3: Estimate the covariance matrix of the observation vector corresponding to each frequency f_n based on these D snap-shots. That is, the ML estimate of the covariance matrix of the observation vector at the frequency f_n is computed from

$$\hat{\mathbf{R}}_y(\omega_n) = \frac{1}{D} \sum_{d=1}^D \mathbf{y}_d(\omega_n) \mathbf{y}_d^H(\omega_n) \quad (7)$$

3. Proposed method for DOA estimation

Marcos et al. [22] have proposed the so-called ‘propagator’ method for array signal processing without any eigen-decomposition. The DOA estimation without eigen-decomposition reduces the computational cost. The propagator is a linear operator based on a partition of the steering vectors, and was found to be a very effective tool for estimating the DOAs.

3.1. Proposed method for a uniform linear array

The algorithm developed in this section is an extension of the narrowband method to the wideband case based on the propagator concept applied to the difference matrix between the FB averaged covariance matrix and the Hermitian of the backward covariance matrix. In this algorithm, the noise is assumed to be cylindrically isotropic. The algorithm proposed in this paper is based on the following property satisfied by Hermitian symmetric Toeplitz matrices:

If a square matrix \mathbf{B} is Hermitian symmetric Toeplitz, then (i) $\mathbf{JB}^T\mathbf{J} = (\mathbf{JB})^T = \mathbf{B}$ and (ii) $\mathbf{B} = \mathbf{JB}^*\mathbf{J}$ (the so-called centro-Hermitian property [29]), where \mathbf{J} represents the exchange matrix with ones along the cross diagonal and zeros elsewhere.

When the noise field is cylindrically isotropic, the noise covariance matrix $\mathbf{Q}_\eta(\omega_n)$ is Hermitian symmetric Toeplitz. Therefore, using the above property (ii),

$$\mathbf{Q}_\eta(\omega_n) = \mathbf{JQ}_\eta^*(\omega_n)\mathbf{J} = \mathbf{JQ}_\eta^T(\omega_n)\mathbf{J} \quad \text{for } n = 0, 1, \dots, N-1. \quad (8)$$

The proposed method employs the FB averaging for the covariance matrix of the observation data. The FB averaging [30,31] is defined as

$$\mathbf{R}_{\text{FB}}(\omega_n) \triangleq \frac{1}{2}(\mathbf{R}_z(\omega_n) + \mathbf{JR}_z^*(\omega_n)\mathbf{J}) \quad \text{for } n = 0, 1, \dots, N-1.$$

Assuming that the unknown noise covariance matrix is symmetric Toeplitz as in [24], the proposed scheme can suppress the noise effects on the array structure by taking the difference $\Delta\mathbf{R}(\omega_n)$ between the FB averaged covariance matrix $\mathbf{R}_{\text{FB}}(\omega_n)$ and the Hermitian of the backward covariance matrix $\mathbf{JR}_z^*(\omega_n)\mathbf{J}$. Now, let us define

$$\begin{aligned} \Delta\mathbf{R}_z(\omega_n) &= \mathbf{R}_{\text{FB}}(\omega_n) - (\mathbf{JR}_z^*(\omega_n)\mathbf{J})^H \\ &= \frac{1}{2}(\mathbf{R}_z(\omega_n) + \mathbf{JR}_z^*(\omega_n)\mathbf{J}) - (\mathbf{JR}_z^T(\omega_n)\mathbf{J}) \\ &\quad \text{for } n = 0, 1, \dots, N-1. \end{aligned} \quad (9)$$

For sake of simplicity the following abbreviations are employed in the sequel:

$$\begin{aligned} \Delta_n &\triangleq \Delta\mathbf{R}_z(\omega_n), \quad \mathbf{R}_{zn} \triangleq \mathbf{R}_z(\omega_n), \quad \mathbf{A}_n \triangleq \mathbf{A}(\omega_n), \\ \mathbf{R}_{sn} &\triangleq \mathbf{R}_s(\omega_n), \quad \mathbf{Q}_{\eta n} \triangleq \mathbf{Q}_\eta(\omega_n). \end{aligned}$$

Thus, by substituting (4) in (9), the difference matrix Δ_n corresponding to f_n for $n = 0, 1, \dots, N-1$, can be written as

$$\begin{aligned} \Delta_n &= \frac{1}{2}(\mathbf{A}_n\mathbf{R}_{sn}\mathbf{A}_n^H + \mathbf{Q}_{\eta n} + \mathbf{JA}_n^*\mathbf{R}_{sn}^*(\mathbf{A}_n^*)^H\mathbf{J} + \mathbf{JQ}_{\eta n}^*\mathbf{J}) \\ &\quad - \mathbf{J}(\mathbf{A}_n\mathbf{R}_{sn}\mathbf{A}_n^H)^T\mathbf{J} - \mathbf{JQ}_{\eta n}^T\mathbf{J}. \end{aligned} \quad (10)$$

Substituting (8) in (10), (10) can be rewritten as

$$\Delta_n = \frac{1}{2}[\mathbf{A}_n\mathbf{R}_{sn}\mathbf{A}_n^H + \mathbf{JA}_n^*\mathbf{R}_{sn}^*(\mathbf{A}_n^*)^H\mathbf{J}] - \mathbf{J}(\mathbf{A}_n\mathbf{R}_{sn}\mathbf{A}_n^H)^T\mathbf{J}. \quad (11)$$

Note that the covariance matrix \mathbf{Q}_η of the unknown noise no longer appears in (11). From the definition of the exchange matrix \mathbf{J} and the steering matrix \mathbf{A}_n , it is easy to verify that \mathbf{A}_n satisfies

$$\mathbf{JA}_n^* = \mathbf{A}_n\mathbf{A}_n, \quad (12)$$

where \mathbf{A}_n is the $K \times K$ diagonal matrix with diagonal entries $\lambda_k = \exp(j\omega_n\tau_M(\theta_k))$ for $k = 1, 2, \dots, K$. Using (12), (11) may be simplified to

$$\Delta_n = \frac{1}{2}[\mathbf{A}_n\mathbf{R}_{sn}\mathbf{A}_n^H - \mathbf{A}_n\mathbf{A}_n\mathbf{R}_{sn}^*\mathbf{A}_n^*\mathbf{A}_n^H] \quad \text{for } n = 0, 1, \dots, N-1. \quad (13)$$

Now we apply the propagator method of [22] to (13). We first give the definition of the propagator. The $K \times K$ sub-matrix \mathbf{A}_{1n} comprising the first K rows of the $M \times K$ steering matrix \mathbf{A}_n is non-singular (full rank) because of the Vandermonde structure of \mathbf{A}_{1n}^H . Therefore, anyone of the remaining $M-K$ rows of the steering matrix \mathbf{A}_n can be expressed as a linear combination of the first K rows. Denoting by \mathbf{A}_{2n} the $(M-K) \times K$ sub-matrix (of \mathbf{A}_n) comprising these remaining $M-K$ rows, we may write $\mathbf{A}_{2n} = \mathbf{P}_n^H\mathbf{A}_{1n}$ where $\mathbf{P}_n^H(\triangleq \mathbf{P}_n^H(\omega_n))$ is the $(M-K) \times K$ matrix whose entries are the coefficients of the linear combinations. The Hermitian \mathbf{P}_n of \mathbf{P}_n^H is the $K \times (M-K)$ propagator matrix at the frequency f_n . Thus, we have the partition

$$\mathbf{A}_n = [\mathbf{A}_{1n}^H : \mathbf{A}_{2n}^H]^H = [\mathbf{A}_{1n}^H : \mathbf{A}_{1n}^H\mathbf{P}_n]^H \quad \text{for } n = 0, 1, \dots, N-1. \quad (14)$$

Using (14), we can partition Δ_n in (13) as

$$\Delta_n = \frac{1}{2} \left\{ \begin{bmatrix} \mathbf{G}_{1n} & \mathbf{G}_{1n}\mathbf{P}_n \\ \mathbf{P}_n^H\mathbf{G}_{1n} & \mathbf{P}_n^H\mathbf{G}_{1n}\mathbf{P}_n \end{bmatrix} - \begin{bmatrix} \mathbf{G}_{2n} & \mathbf{G}_{2n}\mathbf{P}_n \\ \mathbf{P}_n^H\mathbf{G}_{2n} & \mathbf{P}_n^H\mathbf{G}_{2n}\mathbf{P}_n \end{bmatrix} \right\}, \quad (15)$$

where $\mathbf{G}_{1n} = \mathbf{A}_{1n}\mathbf{R}_{sn}\mathbf{A}_{1n}^H$ and $\mathbf{G}_{2n} = \mathbf{A}_{1n}\mathbf{A}_n\mathbf{R}_{sn}^*\mathbf{A}_n^*\mathbf{A}_{1n}^H$. Defining

$$\begin{aligned} \mathbf{G}_n &\triangleq \frac{1}{2} \begin{bmatrix} (\mathbf{G}_{1n} - \mathbf{G}_{2n}) \\ \mathbf{P}_n^H(\mathbf{G}_{1n} - \mathbf{G}_{2n}) \end{bmatrix} \quad \text{and} \\ \mathbf{H}_n &\triangleq \frac{1}{2} \begin{bmatrix} (\mathbf{G}_{1n} - \mathbf{G}_{2n})\mathbf{P}_n \\ \mathbf{P}_n^H(\mathbf{G}_{1n} - \mathbf{G}_{2n})\mathbf{P}_n \end{bmatrix} = \mathbf{G}_n\mathbf{P}_n, \end{aligned}$$

(15) can be expressed as

$$\Delta_n = [\mathbf{G}_n \ \mathbf{H}_n] \quad \text{for } n = 0, 1, \dots, N-1, \quad (16)$$

where \mathbf{G}_n and \mathbf{H}_n are matrices of dimensions $M \times K$ and $M \times (M-K)$, respectively. Considering (16) to define a partition of the difference matrix Δ_n computed on the basis of (9), the relation

$$\mathbf{H}_n = \mathbf{G}_n\mathbf{P}_n \quad (17)$$

between the sub-matrices \mathbf{G}_n and \mathbf{H}_n may not be satisfied in practice since the actual covariance matrix \mathbf{R}_{zn} (which is not available) has to be approximated by the corresponding time auto-covariance matrix $\hat{\mathbf{R}}_{zn}$ which is in turn estimated from a finite number of snap-shots according to (7). However, a least-squares solution for the entries of the propagator matrix \mathbf{P}_n satisfying the overdetermined

system of linear equations (17) may be obtained by minimizing the cost functions

$$J(\mathbf{P}_n) = \|\mathbf{H}_n - \mathbf{G}_n \mathbf{P}_n\|_F^2 \quad \text{for } n = 0, 1, \dots, N-1,$$

where $\|\cdot\|_F$ denotes the Frobenius norm. The cost functions $J(\mathbf{P}_n)$ for $n = 0, 1, \dots, N-1$, being quadratic (convex) functions of \mathbf{P}_n , may be minimized to give the unique least-squares solution for \mathbf{P}_n :

$$\mathbf{P}_n = (\mathbf{G}_n^H \mathbf{G}_n)^{-1} \mathbf{G}_n^H \mathbf{H}_n \quad \text{for } n = 0, 1, \dots, N-1. \quad (18)$$

All the N propagators \mathbf{P}_n for $n = 0, 1, \dots, N-1$, corresponding to the N frequency components, are thus obtained. The computational cost incurred for determining \mathbf{P}_n is less than that incurred in a search for the eigen-elements of a covariance matrix. This has been clearly demonstrated in [22]. The eigen-decomposition entails computational complexity of order $(M^3 + M^2 D)$. The propagator method can reduce the computational complexity to order (MDK) where M , D and K are the number of sensors, the number of snapshots and the number of sources, respectively.

The next key step would be the construction of the transformation (focusing) matrices, $\mathbf{T}_n(\underline{\Delta} \mathbf{T}(\omega_n))$ for $n = 1, 2, \dots, N-1$, that are used to transform the incoherent propagator matrices \mathbf{P}_n for $n = 1, 2, \dots, N-1$, to a pre-selected propagator matrix at the focusing frequency f_0 . Let $Q \leq \min(K, M-K)$. The $Q \times Q$ focusing matrices \mathbf{T}_n for $n = 1, 2, \dots, N-1$ are constructed such that

$$\mathbf{P}_0 = \begin{cases} \mathbf{T}_n \mathbf{P}_n & \text{if } Q = K, \\ \mathbf{P}_n \mathbf{T}_n & \text{if } Q = M - K, \end{cases} \quad (19)$$

for $n = 1, 2, \dots, N-1$. Once again, the least-squares solution of (19) for \mathbf{T}_n is given by

$$\mathbf{T}_n = \begin{cases} \mathbf{P}_0 \mathbf{P}_n^H (\mathbf{P}_n \mathbf{P}_n^H)^{-1} & \text{if } Q = K, \\ (\mathbf{P}_n^H \mathbf{P}_n)^{-1} \mathbf{P}_n^H \mathbf{P}_0 & \text{if } Q = M - K, \end{cases} \quad (20)$$

for $n = 1, 2, \dots, N-1$. The propagators are then combined using these focusing matrices to deliver the focused propagator

$$\mathbf{P}_{\text{foc}} = \begin{cases} \frac{1}{N} \sum_{n=0}^{N-1} \mathbf{T}_n \mathbf{P}_n & \text{if } Q = K, \\ \frac{1}{N} \sum_{n=0}^{N-1} \mathbf{P}_n \mathbf{T}_n & \text{if } Q = M - K, \end{cases}$$

with $\mathbf{T}_0 = \mathbf{I}_Q$ where \mathbf{I}_Q is the $Q \times Q$ identity matrix. If the focusing matrices \mathbf{T}_n , $n = 1, 2, \dots, N-1$, satisfied (19) exactly (possible only when $M = 2K$), then

$$\mathbf{P}_{\text{foc}} = \mathbf{P}_0.$$

If, in addition, the propagator matrices \mathbf{P}_n , $n = 0, 1, \dots, N-1$, satisfied (17) exactly, then (14) for $n = 0$, implies that

$$\mathbf{V}_{\text{foc}}^H \mathbf{A}_0 \underline{\Delta} [\mathbf{P}_{\text{foc}}^H - \mathbf{I}_{M-K}] \mathbf{A}_0 = \mathbf{0}, \quad (21)$$

where $\mathbf{0}$ is the $(M-K) \times K$ matrix of zeros. Now, given a steering matrix $\mathbf{A}_0 = \mathbf{A}(\omega_0) = [\mathbf{a}(\theta_1, \omega_0), \mathbf{a}(\theta_2, \omega_0), \dots, \mathbf{a}(\theta_K, \omega_0)]$, the above Eq. (21) becomes

$$\mathbf{V}_{\text{foc}}^H \mathbf{a}(\theta_k, \omega_0) = \mathbf{0} \quad \text{for } k = 1, 2, \dots, K. \quad (22)$$

Condition (22) suggests that the DOAs of the K wideband sources can be estimated by locating the K largest peaks of

the function

$$F(\theta) = \frac{1}{\mathbf{a}^H(\theta, \omega_0) \mathbf{V}_{\text{foc}} \mathbf{V}_{\text{foc}}^H \mathbf{a}(\theta, \omega_0)}, \quad \theta \in [0, \pi] \quad (23)$$

This approach can be adopted even for the case of spatially white noise.

3.2. Proposed method for an L-shaped array

For 2-D DOA estimation problems, pair matching of elevation and azimuthal angles is necessary. Some of the existing methods to do this requires a complex 2-D search [32–34]. On the other hand, the automatically paired algorithms proposed in [35] need less computation. But it fails when the azimuthal and elevation angles are close to 0° [34] because the argument of the arccosine can then exceed unity. This paper proposes a new method of 2-D DOA estimation for an L-shaped array based on the PM. The proposed method does not suffer from any other problems associated with pair matching.

3.2.1. Estimation of the elevation angle θ

In automatic pair matching, the elevation angle is independent of the azimuthal angle but the azimuthal angle depends on the elevation angle. Thus, estimation of the elevation angle is a 1-D DOA estimation problem. The method adopted for the 1-D case (see Section 3.1) can be used for estimating θ .

3.2.2. Estimation of azimuthal angle φ

The estimate $\hat{\theta}$ of θ will be used to estimate the azimuthal angle φ . The same procedure used to eliminate the noise covariance matrix in Section 3.1 is applied on $\mathbf{R}_x(\omega_n)$ to eliminate the noise covariance matrix $\mathbf{Q}_{\text{px}}(\omega_n)$ from (6). Following exactly the steps outlined in Section 3.1, we obtain expressions for the difference matrix $\underline{\Delta} \mathbf{R}_x(\omega_n)$, the propagator matrices \mathbf{P}_{xn} ($n = 1, 2, \dots, N-1$), the focusing matrices \mathbf{T}_{xn} ($n = 1, 2, \dots, N-1$), and the focused propagator $\mathbf{P}_{x,\text{foc}}$ in complete analogy with those for \mathbf{A}_n , \mathbf{P}_n , \mathbf{T}_n and \mathbf{P}_{foc} derived in Section 3.1 except for the replacement of $\tau_M(\theta_k)$ by $\tau_M(\theta_k, \varphi_k)$ in the expression for the entries λ_k , $k = 1, 2, \dots, K$, of the diagonal matrix \mathbf{A}_n appearing in (12). Making use of the estimates $\hat{\theta}_k$, $k = 1, 2, \dots, K$, of the elevation angles of the K sources obtained as the maxima (with respect to θ) of the objective function $F(\theta)$ defined in (23), the K objective functions required for estimating the associated azimuthal angles φ_k , $k = 1, 2, \dots, K$, are given by

$$F_{\text{cpm}}^{(k)}(\varphi) = 1 / [\mathbf{a}^H(\hat{\theta}_k, \varphi, \omega_0) \mathbf{V}_{x,\text{foc}} \mathbf{V}_{x,\text{foc}}^H \mathbf{a}(\hat{\theta}_k, \varphi, \omega_0)]$$

for $k = 1, 2, \dots, K$,

where $\mathbf{V}_{x,\text{foc}} = [\mathbf{P}_{x,\text{foc}}^H : -\mathbf{I}_{M-K}]$. The estimate $\hat{\varphi}_k$ of φ_k for $k = 1, 2, \dots, K$ is obtained as the global maximum of the objective function $F_{\text{cpm}}^{(k)}$ with respect to φ .

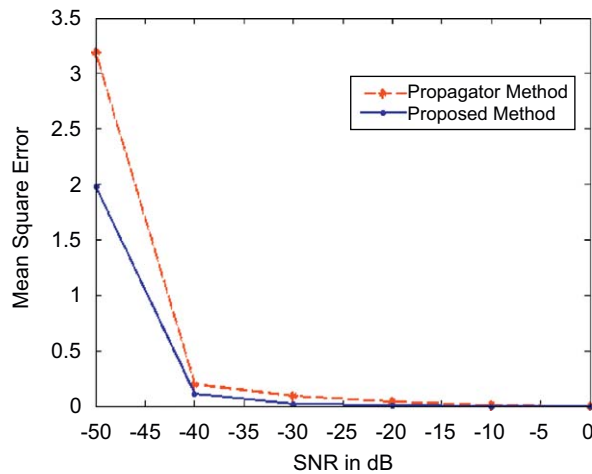
4. Simulation results

In this section, we investigate the performance of the coherent PM using CSSM and the proposed method in terms of the performance indices: (i) mean squared error

Table 1

Specifications used in the simulations.

Number of array elements (M)	7
Signal bandwidth	1 MHz (0.5–1.5 MHz)
Sampling frequency	4 MHz
Number of frequency bins (N)	10
Number of blocks (D)	10
Block length (L)	100

**Fig. 2.** Mean square error versus SNR for a uniform linear array.

(MSE), (ii) resolution capability, (iii) detection probability, (iv) capability to resolve two nearby sources and (v) minimum resolvable angular separation. Computer simulations have been carried out using Matlab 7.0.4 to evaluate the performance of the proposed method for both uniform-linear and L-shaped arrays.

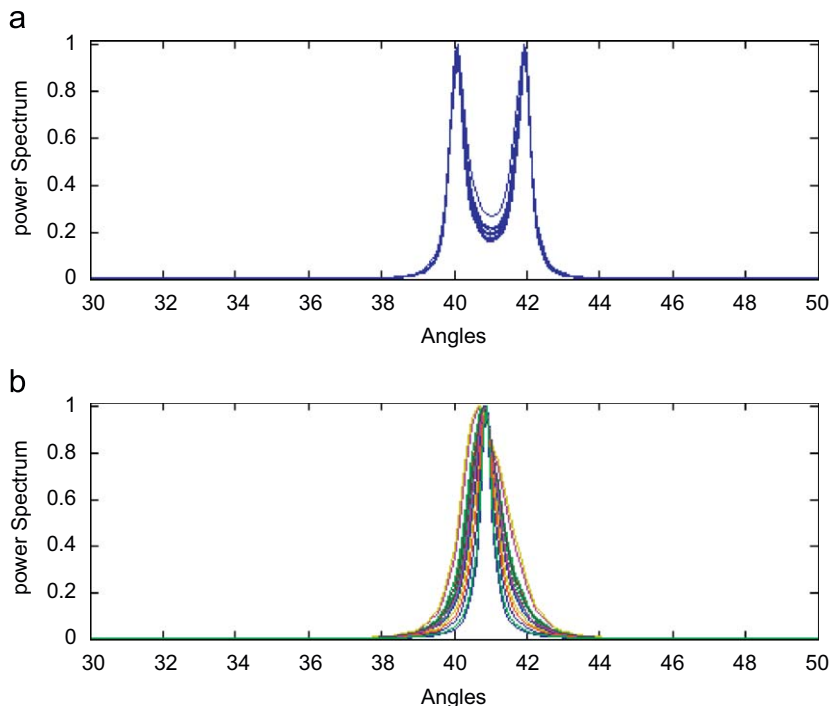
4.1. Performance analysis of the DOA estimation for ULA

In all the simulations, a uniform linear array consisting of uncorrelated omni-directional sensors with a half-wavelength (corresponding to the maximum frequency in the wideband signal) spacing is used, and for each source, the same level of signal power is considered for all the frequency components. Table 1 shows the specifications used in the simulations. The MSE is computed using the formula

$$\text{MSE} = \frac{1}{n} \sum_{i=1}^n (\theta - \hat{\theta}_i)^2,$$

where n is number of trials and $\hat{\theta}_i$ is the DOA estimate of the actual direction θ for the i th trial.

In the first experiment, one source with direction-of-arrival at 45° and a ULA of seven sensors is considered. Simulations have been performed on the propagator and the proposed method for specifications given in Table 1 at different SNR values. The MSE is computed by averaging over 100 independent trials. The MSE versus SNR is

**Fig. 3.** Power spectrum plots of two sources from the directions $\theta = 40^\circ$ and 42° at an equal SNR of 0 dB. (a) For the proposed method and (b) for the coherent propagator method.

plotted for both the methods and the plots are shown in Fig. 2.

In the second experiment, the resolution capabilities of both methods for the case of two signal sources separated by 2° in elevation at an equal SNR of 0 dB are considered. The power spectrum graphs, when the bearing angles of the two sources both lie in the range $[40^\circ, 140^\circ]$, are plotted for 15 trials and are shown in Figs. 3(a)–5(a) for the proposed method and in Figs. 3(b)–5(b) for the coherent propagator method. The power spectrum graphs show that the proposed method resolves the two sources consistently in all the 15 trials while the propagator method does not resolve consistently in every trial.

In the third experiment, the resolution capabilities of both methods for three signal sources from the directions $\theta = 60^\circ, 70^\circ$ and 80° at 0, -2 and 0 dB, respectively, are considered and the power spectrum graphs are plotted for 15 independent trials and are shown in Fig. 6(a) and (b), respectively, for the proposed method and the coherent propagator method. The plots attest to the consistent performance of the proposed method.

Fig. 7 shows the detection probability of second source at an angular separation that is varied between 1° and 9° in the vicinity of first source. The detection probability curves show that the proposed method is capable of resolving two sources separated by an angle of 2° successfully but the propagator method is not able to do so.

Furthermore, the robustness with respect to the number of sources is also analyzed through simulations.

Fig. 8 shows the performance with respect to the number K of distinct sources at an SNR of 0 dB for each source at an angular separation of 10° between adjacent sources. The detection probability is plotted against the number of distinct sources and is shown in Fig. 8, which clearly shows that the proposed method is capable of detecting up to five sources separated by 10° . In contrast, the normal coherent method is able to detect only up to two sources.

Fig. 9 illustrates the performance of both the methods at different SNR values. It depicts the detection probability of a second source at various SNRs from -20 to 0 dB in the vicinity of a first source at 0 dB. It is very clear from Fig. 9 that the proposed method is capable of detecting weak sources in the vicinity of strong ones.

4.2. Performance analysis of the DOA estimation for the L-shaped array

All the simulations for this case are carried out considering the two constituent ULAs with each consisting of seven omni-directional sensors at half-wavelength spacing. The other specifications are same as those given in Table 1. The MSE for this case is computed using the following:

$$\text{MSE} = \frac{1}{n} \sum_{i=1}^n [(\theta - \hat{\theta}_i)^2 + (\varphi - \hat{\varphi}_i)^2],$$

where $(\hat{\theta}_i, \hat{\varphi}_i)$ is the DOA estimate corresponding to the actual direction (θ, φ) for the i th trial.

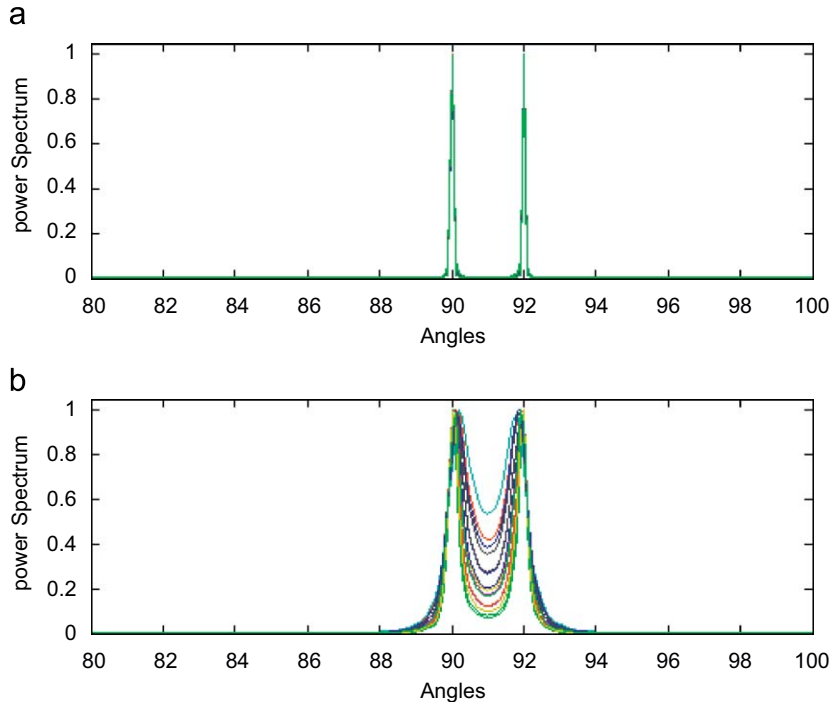


Fig. 4. Power spectrum plots of two sources from the directions $\theta = 90^\circ$ and 92° at an equal SNR of 0 dB. (a) For the proposed method and (b) for the coherent propagator method.

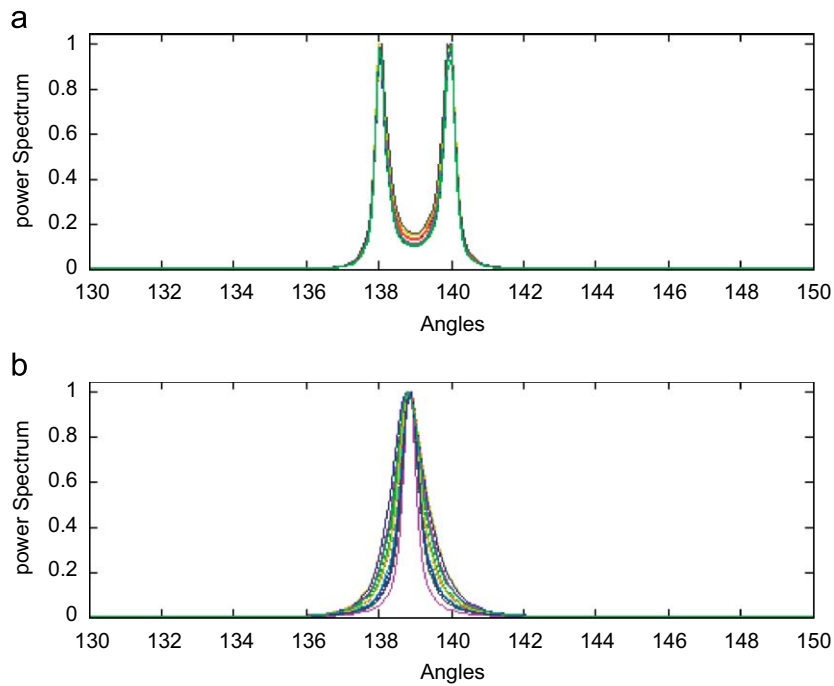


Fig. 5. Power spectrum plots of two sources from the directions $\theta = 138^\circ$ and 140° at an equal SNR of 0 dB. (a) For the proposed method and (b) for the coherent propagator method.

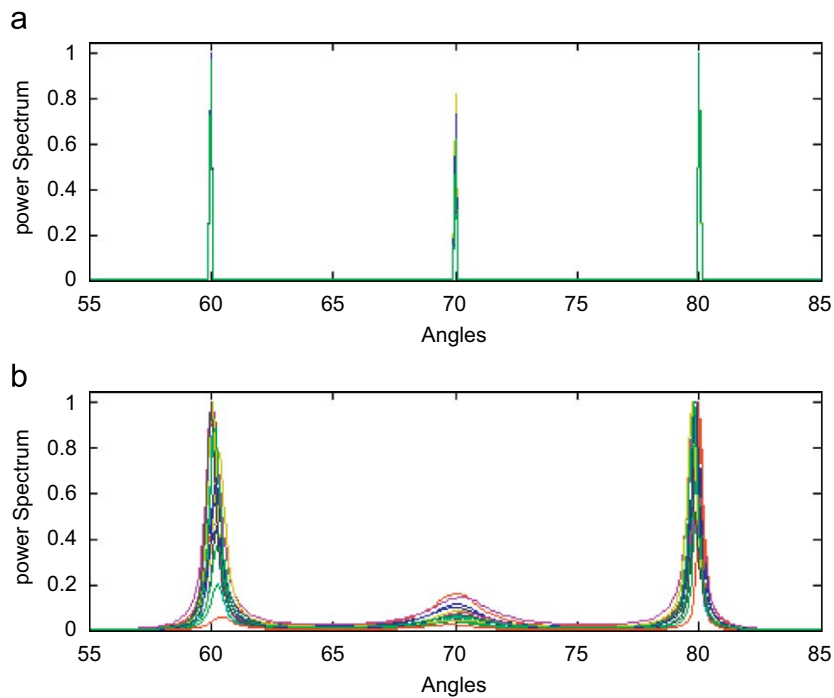


Fig. 6. Power spectrum plots of three sources from the directions $\theta = 60^\circ$, 70° and 80° at 0, -2 and 0 dB. (a) For the proposed method and (b) for the coherent propagator method.

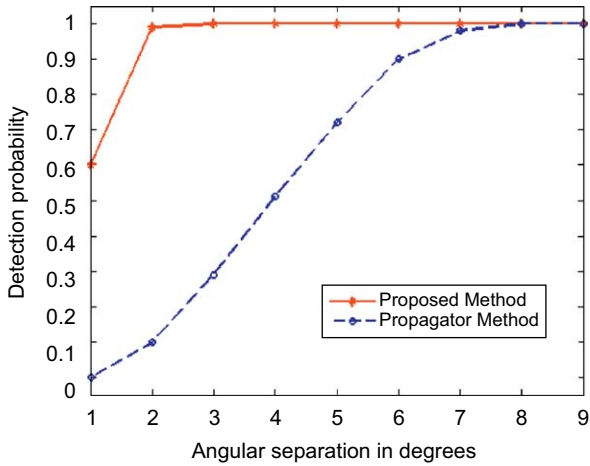


Fig. 7. Detection probability versus angular separation.

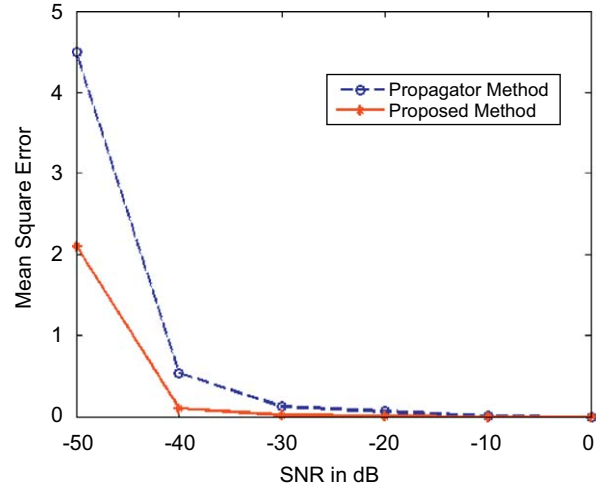


Fig. 10. Mean square error versus SNR for an L-shaped array.

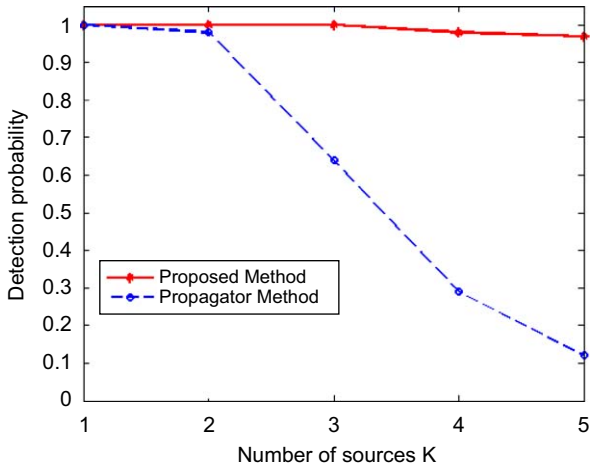


Fig. 8. Detection probability versus number of distinct sources.

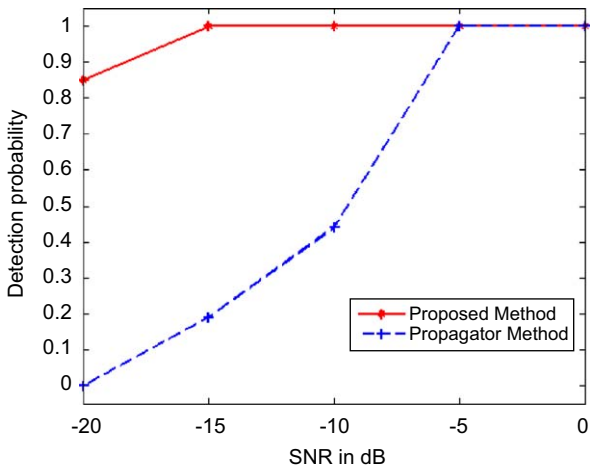


Fig. 9. Detection probability of second source at different SNRs.

In the first experiment, a source at $(45^\circ, 90^\circ)$ is considered and simulations are performed over 100 independent trials for both the methods and the MSE is computed. The MSE versus SNR is plotted for both the methods and plots are shown in Fig. 10.

In the next experiment, the resolution capability of both the methods for two signal sources at $(50^\circ, 125^\circ)$ and $(52^\circ, 126^\circ)$, with an equal SNR of 0 dB, are considered and the power spectrum graphs for both elevation and azimuthal angles are plotted for 15 independent trials and are shown in Fig. 11(a) and (b), respectively, for the proposed method and the coherent propagator method. Fig. 11 depicts that the proposed method performs pair matching successfully while the propagator method fails to do so.

5. Conclusions

In this paper, a new algorithm, which has better resolution capability than the coherent propagator method, and which does not require any eigen-decomposition, is presented for the case of spatially correlated unknown noise fields. The use of the difference between the FB averaged covariance matrix and the Hermitian of the backward covariance matrix is the key step in the method. The propagator method (which does not require any eigen-decomposition) is then applied to the difference matrix. Simulation studies reveal that the performance of the proposed method is superior to that of the propagator method in resolving distinct-power sources as well as in detecting weak sources in the vicinity of strong ones. The unique property of the proposed method for detecting a finite number of sources with an angular separation of 10° has been demonstrated through simulations. It is also seen from the simulation results that the proposed method delivers estimates with less MSE than the propagator method. The computational time for the proposed method is approximately same as that for the propagator method, but the resolution capability of the

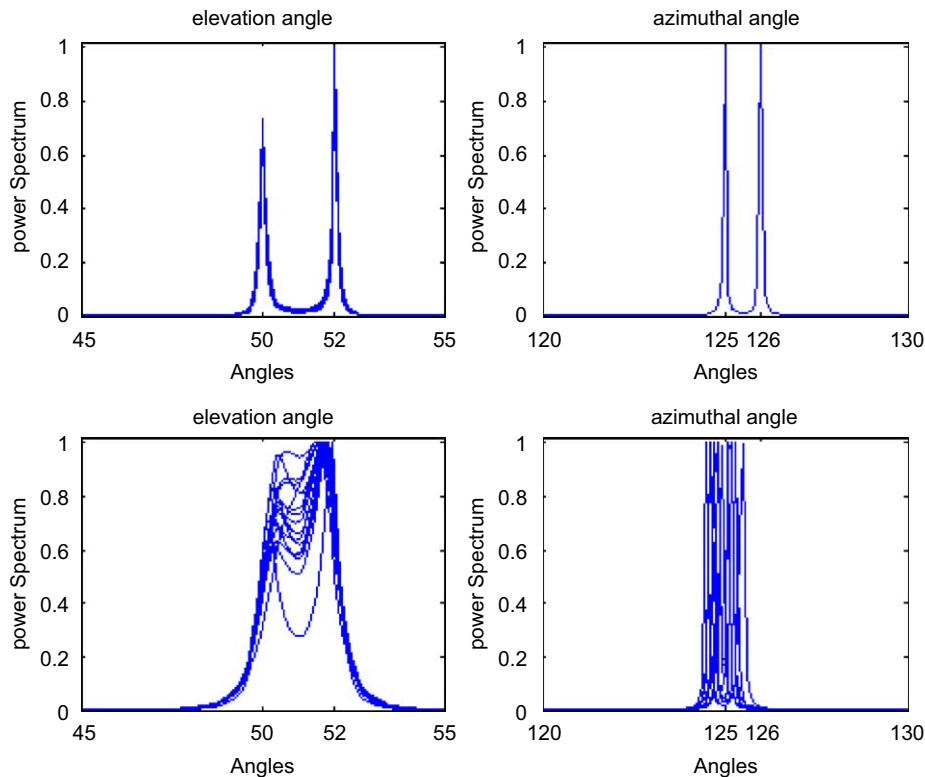


Fig. 11. Power spectrum plots of two sources from the direction $(\theta, \varphi) = (50^\circ, 125^\circ)$ and $(52^\circ, 126^\circ)$ at an equal SNR of 0 dB. (a) For the proposed method and (b) for the coherent propagator method.

proposed method is far superior to that of the propagator method.

References

- [1] H. Krim, B. Ottersten, Two decades of array signal processing research: the parametric approach, *IEEE Signal Process. Mag.* 13 (7) (1996) 67–94.
- [2] R. Schmidt, Multiple emitter location and signal parameter estimation, *IEEE Trans. Antennas Propag.* 34 (4) (1986) 276–280.
- [3] R. Roy, T. Kailath, ESPRIT—estimation of signal parameters via rotational invariance techniques, *IEEE Trans. Signal Process.* 37 (7) (1989) 984–995.
- [4] M. Hussain, Ultra-wideband impulse radar—an overview of the principles, *IEEE AES Syst. Mag.* (9) (1998) 9–14.
- [5] M. Win, R. Scholtz, Ultra-wide bandwidth time-hopping spread spectrum impulse radio for wireless multiple-access communications, *IEEE Trans. Commun.* 48 (4) (2000) 679–691.
- [6] D. Lake, Harmonic phase coupling for battlefield acoustic target identification, in: *Proceedings of IEEE Acoustics Speech and Signal Processing (ICASSP98)*, Seattle, WA, May 1998.
- [7] S. Lehman, A. Devaney, Transmission mode time-reversal super-resolution imaging, *J. Acoust. Soc. Am.* 113 (5) (2003) 2742–2753.
- [8] M. Agrawal, S. Prasad, Broadband DOA estimation using spatial-only modeling of array data, *IEEE Trans. Signal Process.* 48 (3) (2000) 663–670.
- [9] K. Buckley, L. Griffiths, Broad-band signal-subspace spatial-spectrum (BASS-ALE) estimation, *IEEE Trans. Acoust. Speech Signal Process.* 36 (7) (1988) 953–964.
- [10] M. Wax, T. Kailath, Spatio-temporal spectral analysis by eigenstructure methods, *IEEE Trans. Acoust. Speech Signal Process.* 32 (8) (1984) 817–827.
- [11] D. Swingler, J. Krolik, Source location bias in the coherently focused high-resolution broad-band beamformer, *IEEE Trans. Acoust. Speech Signal Process.* 37 (1) (1989) 143–145.
- [12] S. Valaee, B. Champagne, P. Kabal, Localization of wideband signals using least-squares and total least-squares approaches, *IEEE Trans. Signal Process.* 47 (5) (1999) 1213–1222.
- [13] S. Valaee, P. Kabal, Wideband array processing using a two-sided correlation transformation, *IEEE Trans. Signal Process.* 43 (1) (1994) 160–172.
- [14] F. Sellone, Robust auto-focusing wideband DOA estimation, *Signal Process.* 86 (2006) 17–37.
- [15] M. Agarwal, S. Prasad, Estimation of directions of arrival of wideband and wideband spread sources, *Signal Process.* 87 (2007) 614–622.
- [16] H. Wang, M. Kaveh, Coherent signal-subspace processing for the detection and estimation of angles of arrival of multiple wide-band sources, *IEEE Trans. Acoust. Speech Signal Process.* 33 (8) (1984) 823–831.
- [17] G. Gelli, L. Izzo, Cyclostationarity based coherent methods for wideband-signal source location, *IEEE Trans. Signal Process.* 51 (10) (2003) 2471–2482.
- [18] H. Chen, J. Zhao, Coherent signal-subspace processing of acoustic vector sensor array for DOA estimation of wideband sources, *Signal Process.* 85 (2005) 837–847.
- [19] A. El-Keyi, T. Kirubarajan, Adaptive beamspace focusing for direction of arrival estimation of wideband signals, *Signal Process.* 88 (2008) 2063–2077.
- [20] H.V. Trees, *Optimum Array Processing*, Wiley, New York, 2002.
- [21] A. Paulrja, T. Kailath, Eigenstructure methods for direction of arrival estimation in the presence of unknown noise fields, *IEEE Trans. Signal Process.* 34 (1) (1986) 13–20.
- [22] S. Marcos, A. Marsal, M. Benidir, The propagator method for source bearing estimation, *Signal Process.* 42 (1994) 121–138.
- [23] R.J. Talham, Noise correlation functions for anisotropic noise field, *J. Acoust. Soc. Am.* 69 (1) (1981) 213–215.
- [24] S. Prasad, R.T. Williams, A.K. Mahalanabis, L.H. Sibul, A transform-based covariance differencing approach for some classes of parameter estimation problems, *IEEE Trans. Signal Process.* 36 (5) (1988) 631–641.

- [25] R.E. Hernaman, High resolution adaptive array processing—a review of algorithms and performance, in: *Proceedings of the IEE Colloquium on Digital Processing for SONAR*, vol. 30(4), 1985, pp. 3/1–3/4.
- [26] M. Wax, T. Kailath, Detection of signals by information theoretic criteria, *IEEE Trans. Acoust. Speech Signal Process.* 33 (4) (1985) 387–392.
- [27] G. Xu, R.H. Roy, T. Kailath, Detection of number sources via exploitation of centro-symmetry property, *IEEE Trans. Signal Process.* 42 (1) (1994) 102–112.
- [28] Y. Wu, K.W. Tam, On determination of the number of signals, in: *Proceedings of International Conference on Signal and Image Processing*, Honolulu, Hawaii, August 2001, pp. 113–117.
- [29] R. Hill, R. Bates, S. Waters, On centrohermitian matrices, *SIAM J. Matrix Anal. Appl.* 11 (1) (1990) 128–238.
- [30] S. Pillai, B. Kwon, Forward–backward spatial smoothing techniques for the coherent signal identification, *IEEE Trans. Acoust. Speech Signal Process.* 37 (January 1989) 8–15.
- [31] D.A. Linebarger, R.D. DeGroat, E.M. Dowling, Efficient direction-finding method employing forward–backward averaging, *IEEE Trans. Signal Process.* 42 (8) (1994) 2136–2145.
- [32] A. Swindlehurst, T. Kailath, Azimuth-elevation direction finding using regular array geometries, *IEEE Trans. Aerosp. Electron. Syst.* 29 (1) (1993) 1828–1832.
- [33] J.E. Fernández del Río, M.F. Cátedra-pérez, The matrix pencil method for two-dimensional direction of arrival estimation employing an L-shaped array, *IEEE Trans. Antennas Propag.* 45 (11) (1997).
- [34] S. Kikuchi, Tsuji, A. Sano, Pair-matching for estimating 2-D angle of arrival with a cross-correlation matrix, *IEEE Antennas Wireless Propag. Lett.* 5 (2006).
- [35] N. Tayem, H.M. Kwon, L-shape 2-dimensional arrival angle estimation with propagator method, *IEEE Trans. Antennas Propag.* 53 (5) (2004).